EVALUATION OF THE J-INTEGRAL BY ANALYTICAL AND FINITE ELEMENT METHODS

M. H. Bleackley*, A. R. Luxmoore* and J. Sumpter**

***Department of Civil Engineering, University College, Swansea, UK**
****AMTE, Dunfermline, UK**

KEYWORDS

Nonlinear; Fracture Mechanics; Welded Specimens; Plastic Collapse Loads; J_C; Backward Yielding.

ABSTRACT

Numerical and analytical J-integral and load-displacement curves for three point, four point and SENT welded specimens has been compared. The analytical results are good for deep cracks but for shallow cracks, where 'backward' yielding occurs, the analytical results can be unreliable.

INTRODUCTION

Under linear elastic conditions, fracture toughness is represented by such well established fracture parameters as the stress intensity factor K, and its equivalent, the potential energy release rate, G. For most practical engineering materials, whose properties must be determined from relatively small specimens, the linear elastic conditions necessary for valid measurement of either K or G are no longer applicable, as the analysis of the specimens must take into account macroscopic plastic flow surrounding the crack tip. In these test situations, general yield may occur prior to fracture. The problem then arises of how best to characterise the fracture toughness for nonlinear specimen behaviour.

In the current state of the art of nonlinear fracture mechanics, there are two main fracture parameters: the crack opening displacement, COD(BSI, 1972); and the J-integral (Rice, 1968a). Both parameters characterise the crack tip stress field at fracture, but the latter can be more easily determined by analytical and numerical procedures for a given geometry and load in a particular material, and forms the basis of the present study.

The analysis has been restricted to square section, welded specimens containing a through thickness edge crack which varies from shallow to deep and loaded either in 3 point or 4 point bending, or tension. In addition the yield stress of the weld material was varied from an overmatch of the parent metal yield stress to an undermatch.

The J-integral is calculated numerically using a finite element program developed in the Department of Civil Engineering, University College of Swansea, and is compared, where appropriate, to analytical values obtained from an energy method (Sumpter and Turner, 1976) and a displacement method (Bucci, Paris, Landes and Rice, 1972).

In addition to the J-values, various load/displacement curves are obtained numerically and in some cases compared with the analytical and experimental plastic collapse load.

2. ANALYTICAL PLASTIC COLLAPSE LOADS FOR CRACKED SPECIMENS

The analytical plastic collapse loads P_{Lc}, assuming an elastic-perfectly plastic material for the three specimen configurations, take the form

$$P_{Lc} = m\, P_L \tag{1}$$

where P_L is the collapse load for the corresponding uncracked specimen, and m is a constraint factor defined by Haigh and Richard (1974) for the three and four point bend specimens, and Towers and Garwood (1979) for the SENT specimen (the values of m quoted by Haigh and Richards for the SENT specimen appear to be erroneous). The yield stress used is $2\sigma y/\sqrt{3}$ assuming a von Mises yield criterion, where σy is the uniaxial yield stress.

In the three point bend specimens, the localized plastic flow emanating from the central load affects the final collapse load. This effect does not occur in the four point specimens, and it has been observed experimentally (Neal, 1956, pg.229) that the fully plastic moment obtained from the three-point type is somewhat higher than that derived from the latter type for tests on uncracked beams of similar cross section and materials. The actual stress distribution at collapse for the case of a beam with a central concentrated load is more complicated than that envisaged in the simple theory. As contact stresses give rise to a higher collapse load, it can be assured that the longitudinal stresses are reduced in magnitude. Roderick and Phillips (1949) have suggested, from simple elastic theory, that the plastic collapse load for the three point bend specimen be divided by (1-S/W) to take account of the point load.

3. THE J-INTEGRAL CONCEPT

3.1 J Defined as a Contour Integral

Considering a two dimensional nonlinear elastic body in either plane stress or plane strain with a crack aligned in the x direction, Rice (1968a) defined J as:

$$\int_{\Gamma} \left(W dy - T_i \frac{\partial u_i}{\partial x} ds \right) \tag{2}$$

where W is the strain energy density

$T_i = \sigma_{ij} n_j$ is the traction vector defined by the stress tensor σ_{ij} and the outward normal along Γ

u_i is the displacement vector

Γ is any contour from the lower crack face anticlockwise around the crack tip to the upper face

s is the arc length of Γ

3.2 Approximating J as a Function of Energy

Sumpter and Turner (1976) have suggested that J can be decoupled into its elastic and plastic components, in the same way as the potential energy can be decoupled into its elastic (U^e) and plastic (U^p) components.

$$J = J_e + J_p$$
$$= \eta_e \frac{U^e}{W-a} + \eta_p \frac{U^p}{W-a} \quad (3)$$

where η_e and η_p are constants of geometry, see Turner (1979, Appendix 4) and U^e and U^p are the elastic and plastic energies calculated from load/load point displacement curve.

3.3 Approximating J as a Function of Displacement

An alternative interpretation of J (Rice, 1968b) is that of a potential energy difference for identically loaded configurations having corresponding crack sizes of a and a + Δa, i.e.

$$J = -\frac{1}{B} \left. \frac{U_a - U_{a+\Delta a}}{\Delta a} \right|_\delta = -\frac{1}{B} \left. \frac{\Delta U}{\Delta a} \right|_\delta \quad (4)$$

where ΔU is the difference in energy of the two configurations at a particular load point displacement δ.

Assuming an elastic perfectly plastic load/displacement curve, $U^p = P_{Lc}\ \delta$. Substituting into equation (4), the plastic component of J becomes

$$J_p = -\frac{\delta}{B} \frac{\partial P_{Lc}}{\partial a} \quad (5)$$

where P_{Lc} is defined from equation (1)

For the elastic component J_e is simply related to the stress intensity factor K by

$$J_e = K^2 \frac{(1-\nu^2)}{E} \text{ in plane strain} \quad (6)$$

K calibrations for the three point bend are obtained from Bucci et al,(1972, pg.52) and for the SENT geometries from Towers and Garwood,(1979, p.21). As these calibrations are a function of load, they are computed as functions of displacement by analytical load/displacement expressions obtained from Bucci et al, (1972, pg.50) for the three point bend specimen and Towers and Garwood, (1979, p.21) for the SENT specimen.

4. NUMERICAL PROCEDURE

4.1 Numerical Representation of the Specimens

The specimens in Fig. 1 are 51mm square with crack length/width ratio varying from 0.1 to 0.5. They are modelled using a two-dimensional elastic-plastic finite element program based on small strain incremental theory and the initial stress approach (Zienkiewicz, 1977, pg. 459).

Two finite element meshes were constructed, consisting of 54 and 100 eight noded isoparametric elements. Due to symmetry only one half of the specimen is modelled. The elements of the meshes are arranged so as to accommodate the weld. The coarser mesh is used to model specimens with a/w = 0.147, 0.31, 0.49 and the finer mesh for a/w = 0.098.

The material properties of the specimen are shown in Fig. 2 for both the weld and parent metals. Linear work hardening is assumed for all the metals. The ratio of the parent metal yield stress to the weld metal yield stress varies from an overmatch (1:1.3) through homogeneous (1:1) to an undermatch (1:0.85)

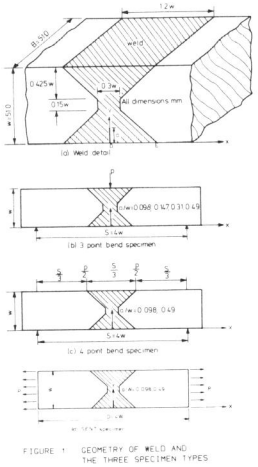

FIGURE 1 GEOMETRY OF WELD AND THE THREE SPECIMEN TYPES

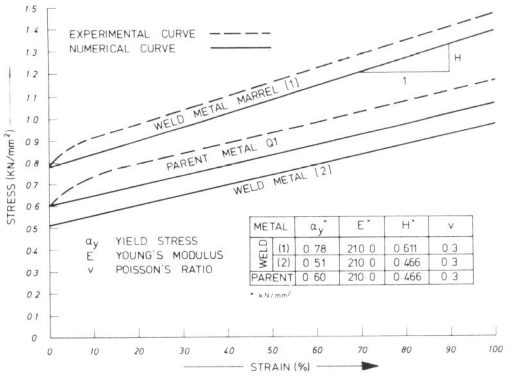

FIGURE 2 STRESS STRAIN CURVES FOR THE WELD AND PARENT METALS OF THE 3 AND 4 POINT BEND SPECIMENS

Figure 1 shows the crack lengths of each particular geometry. Three analyses were done for each crack length to accommodate the three different yield stresses. In addition, computations were carried out on each homogeneous specimen having no crack.

The dimensions of the specimen dictate a plane strain constraint. Von Mises yield criterion was used for all specimens. Loading was by applied displacements.

4.2 Numerical Evaluation of the J-Integral

The J integral is calculated numerically along a contour defined by a line passing through specific Gauss points within the elements and where the stresses and strains have been determined. Defining a segment of the contour as the distance between any two consecutive Gauss points, J is obtained by integrating equation(2), segment by segment in an anticlockwise fashion using the mean values of the stresses and strains at the mid point of each segment.

The J integral is calculated for several different paths encompassing the crack tip and an average value taken. These paths vary from enclosing the near field around the crack tip to the far field at the specimen edges.

To help ascertain if there is any discernible difference between paths which do not pass through the parent metal when a weld is present, some paths were chosen so that they would only pass through the weld material whilst others transversed the weld/parent interface.

In addition to the contours surrounding the crack tip, two closed loops were constructed, in order to obtain some idea of the error involved in numerically determining the J values. This error is readily obtainable, as the J value calculated around a loop enclosing an area free of body forces is zero.

5. NUMERICAL AND ANALYTICAL RESULTS

The following results are obtained from loading the bend and SENT specimens to an arbitrary load point displacement well in excess of plastic collapse.

5.1 Comparison of Numerical and Analytical Load-Displacement Curves

The numerical variation of load-point displacement for the three specimen types show, as expected, the plastic collapse load increasing with the weld metal yield stress and the shallowness of the crack.

A comparison of numerical and analytical values of the plastic collapse loads is given in Table 1 for the homogeneous specimens. The analytical values of the three point bend plastic collapse loads incorporating an adjustment for the point load and compared in Table 1, column 7 with the numerical values, show less variation the deeper the crack. The opposite effect is shown in column 6 of the same table for the comparison of the analytical collapse loads with no adjustment for the point load.

	$a/_W$	m	P_{Lc} (KN)	$P_{Lc}' = \frac{P_{Lc}}{1-\frac{W}{S}}$ (KN)	Approx. Numerical Collapse load P_N (KN)	$\frac{P_N - P_{Lc}}{P_N}$ %	$\frac{P_N - P_{Lc}'}{P_N}$ %
3 PT. BEND SPECIMEN	0	1.0	459.5	616.8	535.0	14.0	- 15.3
	0.098	0.923	421.1	569.3	485.0	12.6	- 17.4
	0.147	0.864	397.1	533.0	465.0	14.6	- 14.6
	0.31	0.581	266.9	358.3	315.0	15.4	- 13.7
	0.49	0.317	145.8	195.7	185.0	21.2	- 5.8
4 PT.BEND SPECIMEN	0	1.0	689.3	NOT	695.0	0.8	NOT
	0.098	0.923	636.5	APPLICABLE	670.0	5.0	APPLICABLE
	0.49	0.328	225.9		260.0	13.0	
SENT SPECIMEN	0	1.0	1802.0	NOT	1800.0	0.1	NOT
	0.098	NOT APPLICABLE	-	APPLICABLE	1700.0	-	APPLICABLE
	0.49	0.51	919.1		1000.0	8.1	

Table 1. Plastic Collapse Load For The Homogeneous, 3 Point, 4 Point and SENT Specimens

The numerical and experimental curves for the variation of load with clip gauge displacement are shown in Fig. 3. These experimental curves are from tests conducted by the Welding Institute (Dawes, 1976, unpublished) on three-point bend specimens with a parent metal to weld metal yield stress of 1:1.3. For the shallow cracked specimens, the experimental and numerical plastic collapse loads compare well, although the elastic compliances do not. The deep cracked specimens failed by brittle fracture, and so no plastic collapse load occured. In these cases the numerical and experimental elastic compliances are in agreement.

The comparison of the numerical and analytic collapse loads for the four point bend specimens in Table 1 is very good for the uncracked specimen, but worsens with increasing crack length.

The analytical and numerical collapse loads are in good agreement for the uncracked and deep cracked SENT specimens. For this geometry the constraint factor of equation(1) is undefined for the shallow crack.

5.2 Numerical J-Values

For the three specimen types, the average value of the J-integral was obtained as a function of load-point displacement (δ) and clip gauge displacement (Vg).

The trend of the J-δ curves for the various crack lengths does not correspond to the J-Vg results, although different weld yield stresses do produce the same relative behaviour in the bend and deep notch tension geometries (Bleackley and Luxmoore, 1979). Figure 4 shows the J/δ and J/Vg relationship for the three point bend specimen.

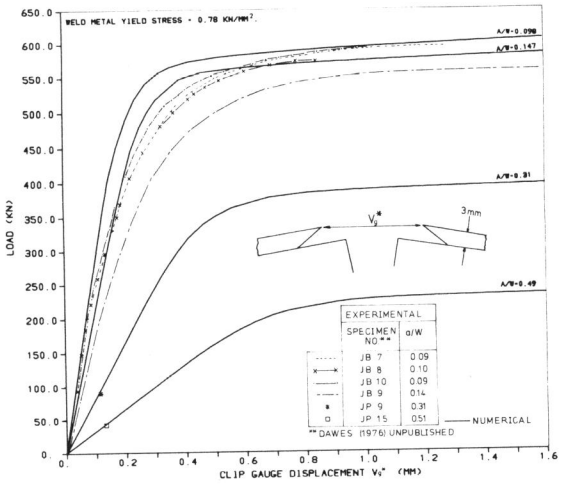

FIGURE 3 NUMERICAL AND EXPERIMENTAL COMPARISON OF LOAD-CLIP GAUGE DISPLACEMENT (V_0^*) CURVES FOR FOUR 3 POINT BEND SPECIMENS. (A/W = 0.098, 0.147, 0.31, 0.49)

Table 2 shows the maximum variation from the mean of two sets of integral paths. Path set A, passes just through the weld material, whilst path set B tranverses the weld/parent interface. The homogeneous results corresponding to the same a/W values are included to give some indication of the numerical error, as the path sets should show no significant variation in this case, as there is no weld.

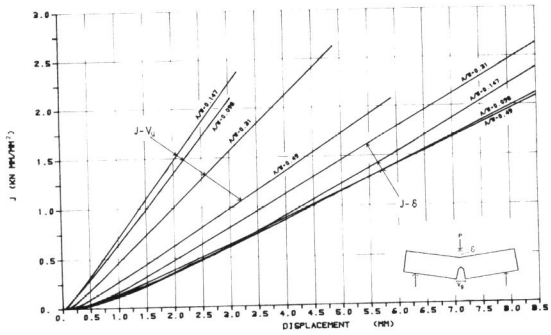

FIGURE 4 VARIATION OF THE J INTEGRAL WITH LOAD POINT DISPLACEMENT(δ) AND CLIP GAUGE DISPLACEMENT(V_0) FOR THE THREE POINT BEND HOMOGENEOUS SPECIMEN WITH VARIOUS A/W VALUES. (54 AND 100 ELEMENT MESHES)

The corresponding homogeneous results included are computed from the exact same data as the nonhomogeneous specimens in terms of load increments etc.

For the four point bend results the variation of paths sets is similar to the homogeneous specimens. For the SENT specimen and to a lesser extent the three point bend specimen , the J paths deviate significantly from the homogeneous results.

The three point bend specimens showed the least path variation of the individual J paths, with a maximum difference from the mean of 10.8%. The four point bend models have a maximum variation of 18.5% and the SENT specimens 16.7%.

The maximum closed loop value is 9.1% of the mean J value for the deep cracked SENT specimen. However, only 14% of all closed loop results for all the specimens produced J values exceeding 3% of the mean J values taken around the crack.

Geometry	Path Set	a/W	Weld Yield Stress KN/mm^2	Maximum Variation From Mean of Path Sets %	Corresponding Equivalent Homogeneous Result For Same a/W Value
3 Pt Bend	A	0.098	0.78	3.8	1.2
	B	0.49	0.78	- 5.8	1.7
4 Pt Bend	A	0.49	0.51	3.1	2.8
	B	0.49	0.51	- 1.0	- 0.9
SENT	A	0.49	0.78	-12.4	- 2.6
	B	0.49	0.78	4.1	0.9

Table 2. Variation Of Path Sets From the Mean J-Value

5.3 Comparison of Numerical and Analytical J Values

The energy method (Sumpter and Turner, 1976) could be used to estimate J-values for all specimen combinations, as it only required estimates of U^e and U^p, (equation 3), whereas the displacement method, (Bucci et al, 1972) strictly could only be applied to the homogeneous specimens, because it was not possible to estimate analytically the collapse load. For the energy method, the writers did not possess sufficient experimental data to determine U^e and U^p, and these values were taken from the numerical computations. It was found (Bleackley and Luxmoore, 1979) that there is very little difference if U^e and U^p are obtained from the numerical load-displacement curve or directly from the numerical energies.

The numerical and analytical values of J for the three point bend and SENT geometries are shown in Figs. 5 to 10. For the three point bend specimen with different welds, J determined analytically (by the energy method) shows good agreement with numerical results for small a/W values. For J determined by the displacement method, the opposite is true.

In one case, the J value was also calculated numerically for the shallow cracked bend specimen from two slightly different crack lengths using equation 4. The agreement between this method and the numerical line integral evaluation was good, Fig. 5.

As the limit load for the shallow notch SENT geometry is undefined, it is only possible to determine J_e and not J_p using the displacement method. Hence the comparison for this geometry must be treated with caution, Fig. 9. The effect of the different yield stress ratios is surprising, and the homogeneous numerical results are significantly different to those obtained by the energy method. For the deep cracked SENT geometry, the correlation of the numerical and two analytical solutions is good, particularly for Sumpter's and Turner's method.

5.4 Backward Yielding

For the shallow crack bend specimens (a/W = 0.098 and 0.147) with homogeneous and

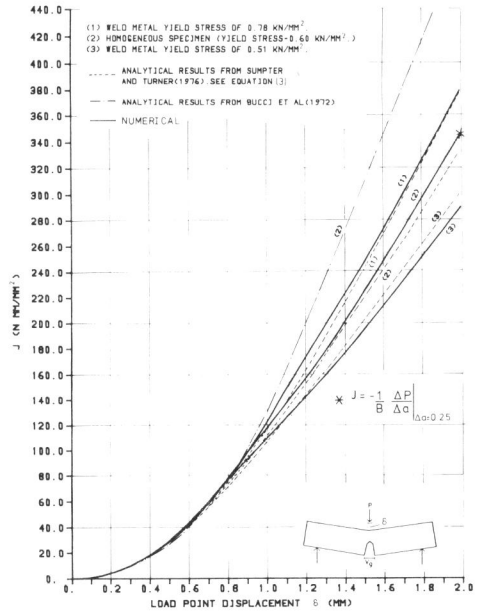

FIGURE 5 NUMERICAL AND ANALYTICAL COMPARISON OF THE J-LOAD POINT DISPLACEMENT CURVE FOR THE 3 POINT BEND SPECIMEN. (A/W=0.098)

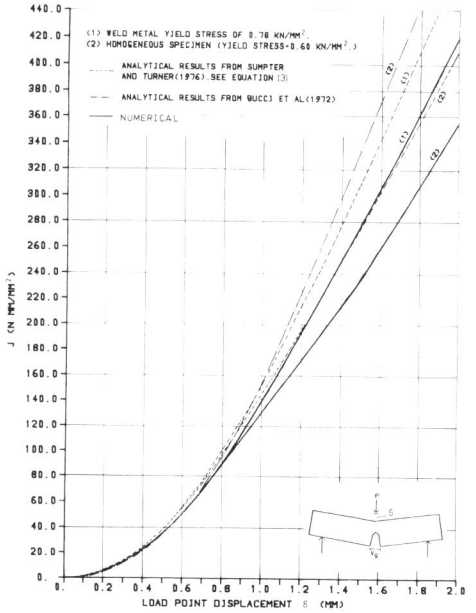

FIGURE 6 NUMERICAL AND ANALYTICAL COMPARISON OF THE J-LOAD POINT DISPLACEMENT CURVE FOR THE 3 POINT BEND SPECIMEN. (A/W=0.147)

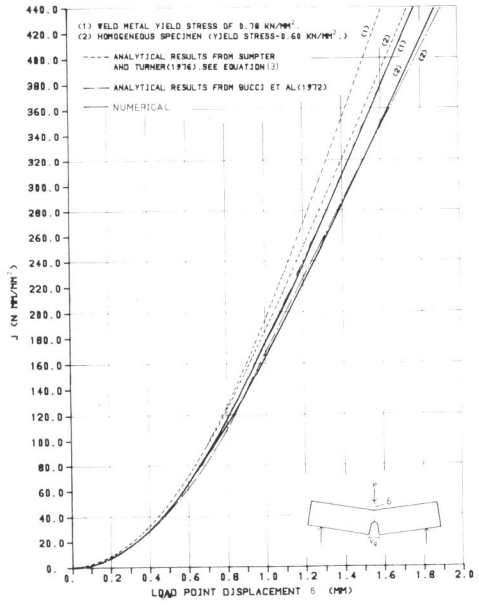

FIGURE 7 NUMERICAL AND ANALYTICAL COMPARISON OF THE J-LOAD POINT DISPLACEMENT CURVE FOR THE 3 POINT BEND SPECIMEN. (A/W=0.31)

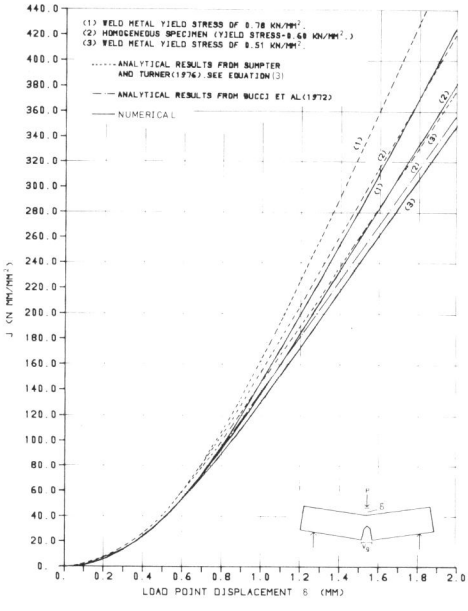

FIGURE 8 NUMERICAL AND ANALYTICAL COMPARISON OF THE J-LOAD POINT DISPLACEMENT CURVE FOR THE 3 POINT BEND SPECIMEN. (A/W=0.49)

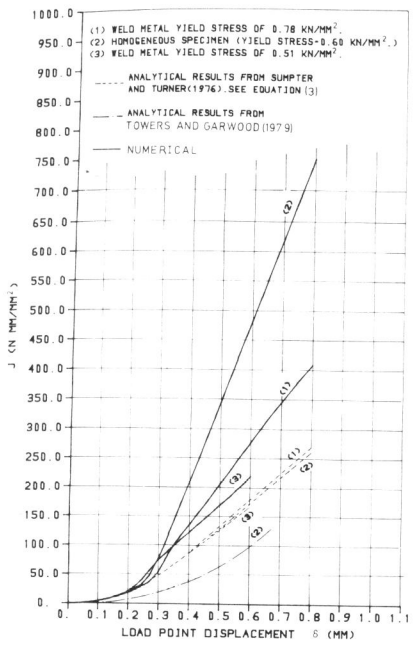

FIGURE 9 NUMERICAL AND ANALYTICAL COMPARISON OF THE J-LOAD PT. DISP. CURVE FOR THE SENT SPECIMEN. (A/W=0.098)

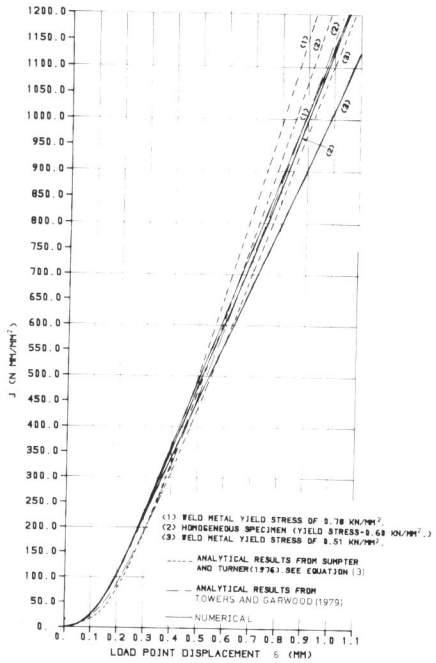

FIGURE 10 NUMERICAL AND ANALYTICAL COMPARISON OF THE J-LOAD PT. DISP. CURVE FOR THE SENT SPECIMEN. (A/W=0.49)

undermatched weld yield stress, the computations showed that plastic flow extended backwards i.e. to the specimen edge where the crack mouth is situated, prior to general yield across the ligament, Fig. 11. For a/W = 0.31, backward yielding occurred just after general yield on the ligament, but no backward yielding was observed for a/W = 0.49. With the overmatched weld metal yield stress, backward yielding occurred at a later stage in the load cycle e.g. for a/W = 0.098, it occurred at approximately the same point as ligament yielding, and it was only observed at very large displacements for a/W = 0.31.

As expected, yielding was confined to the weld region for the undermatched weld metal.

6. COMPARISON WITH EXPERIMENTAL J-VALUES

Experimental J_c values were obtained from the same tests as the load-displacement results on three-point bend specimens with a parent to weld metal yield stress of 1 to 1.3 (Dawes, 1976, unpublished). These experimental results showed that shallow cracks (a/W < 0.15) failed in a mainly ductile fashion, with correspondingly high J_c values, whereas deeper cracks usually failed at loads corresponding to LEFM conditions, with very low J_c values. One possible explanation of this dichotomy of behaviour was the backward extension of plasticity from the crack tip (described in section 5.4) relieving the constraint at the crack tip prior to general yield across the ligament. For a/W > 0.15, backward yielding occurs after general yield across the ligament.

The question arose as to whether the original experimental estimation of J for these specimens reflected this backward yielding, and so the present numerical results were used, in conjunction with the experimental clip gauge displacement at failure, to check some of the experimental J_c values, Table 3. The agreement is reasonable for both the deepest cracks (where virtually no plasticity occurred at failure), and the shallow cracks. It is thus clear that the discrepancy in mechanical behaviour of these two extremes does not lead to consistent J_c values.

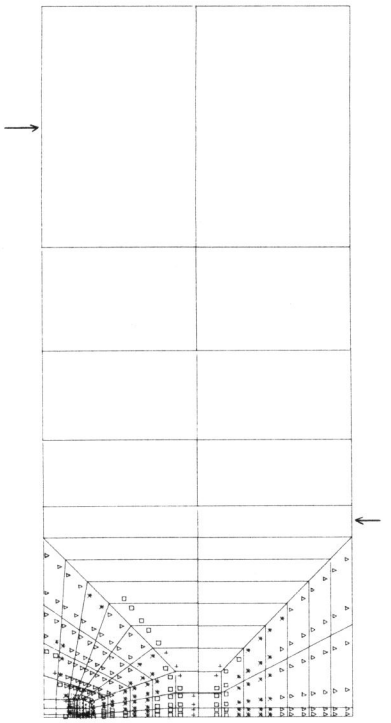

FIGURE 11 PLASTIC ZONE DEVELOPEMENT FOR THE 4 POINT BEND SPECIMEN FOR A/W=0.05E. WELD METAL YIELD STRESS=0.51 KN/MM (100 ELEMENT MESH)
△ LOAD POINT DISPLACEMENT=0.72 MM.
✱ LOAD POINT DISPLACEMENT=1.02 MM.
□ LOAD POINT DISPLACEMENT=1.50 MM.
+ LOAD POINT DISPLACEMENT=2.50 MM.

DISCUSSION

The numerical and analytical plastic collapse loads compare very well for the uncracked SENT and four point bend specimens. For the deep cracked four point bend and SENT specimens, the comparison is not so good.

In the analytical calculations on the three point bend specimen, no adequate proposals appear to have been made for the effect of the central point load. As a consequence the comparison of the numerical and analytical plastic collapse loads for the three point bend specimens are only fair. There is good agreement with the experimental and numerical plastic collapse loads for the three point bend specimens, indicating that the numerical results are realistic. It would seem that the constraint factor m is not sufficiently accurate for an analytical limit load evaluation in this geometry.

The different trends produced by plotting J against clip gauge displacement as opposed to load point displacement can be confusing although the explanation is purely geometrical.

The numerical and analytical J values show reasonable compatibility with the exception of the shallow cracked SENT specimen. With this exception the comparison is reasonable for the parabolic portion of the curve. It is for the linear portion of the J curve (when general yield has occurred) that the discrepancies appear. With the analytical displacement method for determining J, the slope of the curve is dependent on the constraint factor m defining the plastic collapse load of that specimen. If this function is ill defined, as seems the case with the results of some of the load displacement curves, it may not be possible to get good analytical J values.

It should be noted that this function is differentiated with respect to the crack length to determine the slope of the J_p curve for given geometry and material properties and hence the error due to m may not manifest itself to such an extent as in the analytical load-displacement curves.

The numerical results support the contention that backward yielding relieves the constraint at the crack tip, leading to ductile fracture behaviour for the shallow

cracked specimens. Even for a/W = 0.31 backward yielding occurred just after general yield across the ligament, and the additional loss of constraint could produce ductile fracture.

Experimental Specimen *	Experimental a/W	Numerical a/W	Maximum Experimental J Nmm/mm^2	Numerical J Nmm/mm^2 At Corresponding Vg
JP 1	0.10	0.098	1081	922
JP 3	0.15	0.147	939	978
JP 9	0.31	0.31	8.8	9.5
JP 8	0.33	0.31	160	209
IZ 2	0.50	0.49	5.6	5.5
JP 12	0.51	0.49	5.8	5.5
IZ 1	0.51	0.49	7.3	7.5
IZ 5	0.51	0.49	125	150

*(Dawes, 1976, unpublished)

Table 3. Comparison of Numerical and Experimental J Values

REFERENCES

BLEACKLEY, M. H. and Luxmoore, A.R., An Elasto-Plastic Analysis of Cracks in Welds. Progress Report from 1st November, 1978 - 31st October, 1979, University College Swansea.

British Standards Institution (1972) Methods for Crack Opening Displacement (COD) Testing, British Standards Institution Document, DD19, London.

Bucci, R.J., Paris, P.C., Landes, J.D. and Rice, J.R. (1972), J-Integral Estimation Procedures. In: Fracture Toughness Proceedings of the 1971 National Symposium on Fracture Mechanics, Part II, A STM STP 514, pages 40-69, American Society for Testing and Materials.

Haigh, J.R. and Richards, C.E. (1974), Yield Point Loads and Compliance Functions of Fracture Mechanics Specimens. Report No. RD/L/M 461. Central Electricity Generating Board.

Neal, B.G. (1956), Plastic Methods of Structural Analysis. Chapman and Hall, London.

Rice, J.R. (1968a) A path independent integral and the approximate analysis of strain concentration by notches and cracks. Journal of Applied Mechanics (June): 379-386, Transactions of the American Society of Mechanical Engineers.

Rice, J.R. (1968b) Mathematical Analysis in the Mechanics of Fracture. In: Fracture an Advanced Treatise. Volume II, pages 191-311, edited by H. Liebowitz. Academic Press, London.

Roderick, J.W. and Phillips, I.H. (1949). The carrying capacity of simply supported mild steel beams. Research (Engineering Struct. Supplement), Colston Papers, 2(9).

Sumpter, J.D.G. and Turner, C.E. (1976), Method for Laboratory Determination of J_c In: Cracks and Fracture, ASTM STP 601, pages 3-18, American Society for Testing and Materials.

Towers, O.L. and Garwood, S.J. (1979) Ductile Instability Considerations and the Prediction of Driving Force Curves for Six Test Geometries. Report No: 7301/05/79/160.2 Welding Institute, Cambridge, England.

Turner, C.E. (1979), Methods for Post-yield Fracture Safety Assessment. In: Post-Yield Fracture Mechanics.Edited by D.G.H. Latzko Applied Science, London.
Zienkiewicz, O.C. (1977), The Finite Element Method. 3rd Edition, McGraw Hill.